Fe-porphyrin monolayers on ferromagnetic substrates: Electronic structure and magnetic coupling strength

M. Bernien, X. Xu,* J. Miguel, M. Piantek, Ph. Eckhold, J. Luo, J. Kurde, W. Kuch, and K. Baberschke

Institut für Experimentalphysik, Freie Universität Berlin, Arnimallee 14, D-14195 Berlin, Germany

H. Wende† and P. Srivastava‡

Fachbereich Physik, Experimentalphysik-AG Wende, Universität Duisburg-Essen, Lotharstrasse 1, D-47048 Duisburg, Germany

In this work, the different coupling strengths of Fe-octaethylporphyrin molecules sublimated *in situ* onto epitaxially grown Co and Ni films on Cu(100) are studied by systematic x-ray-absorption and x-ray magnetic circular dichroism (XMCD) measurements. The fine structures observed in the absorption and dichroic spectra of the Fe-$L_{2,3}$ edges are explained in terms of different Fe 3d orbitals probed in angular-dependent measurements. The coverage of Fe-porphyrin molecules is varied from submonolayer to 1.5 ML (monolayer), and measurements were carried out at room as well as at low temperatures. From the temperature dependence of the Fe-XMCD signal, a weaker coupling strength between the Fe atom and the Ni substrate is found as compared to the Co case.

I. INTRODUCTION

Porphyrins have attracted the attention of the scientific community for a very long time now. Initially, this interest originated from their biological significance and catalytic capabilities. Lately, 3d metal porphyrins have generated much interest due to their structural and magnetic properties. With technological advancement in various experimental techniques and theoretical codes, there is a substantial increase in the research efforts in this area.[1–11] In addition, recent developments in the field of surface magnetism[12] and possible application of specific porphyrins in molecular spintronics as switchable magnetic molecules[13] have given a new dimension to the studies that investigate their electronic structure and magnetic properties.

In the recent past, porphyrins have been investigated with different techniques.[1–6] Electronic structure calculations have also been performed for bulk samples and free molecules.[7–11,14] However, if one wants to focus on the magnetic properties of porphyrins, a technique such as x-ray magnetic circular dichroism (XMCD) has unique advantages over other techniques because of its element specificity and monolayer sensitivity. Furthermore, the application of sum rules to the XMCD[15,16] is nowadays widely used to determine the local orbital and spin angular moments.

The induced magnetic ordering in a molecular monolayer of Mn(III)-tetraphenylporphyrin-Cl on a thin Co film substrate was studied using XMCD.[6] In contrast to the Mn case, the application of sum rules for Fe is very reliable.[12,17] Recently, we have investigated the structural and magnetic properties of Fe(III)-octaethylporphyrin(OEP)-Cl molecules prepared by sublimation on ferromagnetic substrates using x-ray-absorption (XAS) and XMCD measurements.[18] We observed that the Fe magnetic moment can be switched in plane or out of plane by a magnetization reversal of the substrate. *Ab initio* electronic structure calculations identified a 90° super exchange coupling of the Fe ion to the surface atoms through the N ligands.

In the present work, other aspects of the magnetic coupling of Fe-OEP molecules to Co and Ni ferromagnetic substrates have been tackled. We have carried out systematic XAS and XMCD investigations by preparing different coverages [submonolayer to 1.5 ML (monolayer)] of these molecules on Co and Ni thin films. Single and double ferromagnetic layers in the range of a few atomic MLs were deposited on Cu(100) to have the possibility of aligning the magnetization easy axis in plane and out of plane. We discuss the contribution of the different Fe 3d orbitals to the fine structures observed in the absorption and dichroic spectra. In addition, temperature-dependent measurements were performed in order to quantify the coupling strength between Fe-OEP molecules and both substrates. They were used to estimate the coupling energies for the Co and Ni substrates.

II. EXPERIMENT

The sample preparation was carried out in ultrahigh vacuum conditions ($p=2.0\times10^{-10}$ mbar). The ultrathin Co and Ni films were epitaxially grown by electron-beam evaporation on a Cu(100) single crystal, which was cleaned by repeated Ar$^+$ sputtering and annealing cycles. The Co and Ni layer thicknesses were chosen to be 5 and 15 ML, respectively, in order to obtain in-plane and out-of-plane easy magnetization axes. A combined 5 ML Ni/5 ML Co bilayer was also prepared, displaying in-plane magnetization. In order to reduce the roughness of the Ni films, they were annealed to 420 K prior to the deposition of the molecules.

The porphyrin molecules [2,3,7,8,12,13,17,18-octaethylporphyrin-Fe(III) chloride] were adsorbed on the ferromagnetic films at room temperature by sublimating Fe-OEP-Cl molecules at 485 K. The thicknesses of the porphyrin and ferromagnetic films were determined by a quartz microbalance and medium-energy-electron-diffraction intensity oscillations, respectively, and were cross-checked by the signal-to-background ratio (edge jump) at the respective x-ray-absorption edges.

X-ray-absorption spectroscopy in total electron yield experiments was performed at the beamline UE56-2/PGM2 at BESSY. We used this undulator beamline with a plane grating monochromator to produce circular polarized photons with an energy resolution of about 300 meV and a circular polarization degree of 80% at the energy ranges of the Fe-, Co-, and Ni-$L_{2,3}$ edges. The measurements were done under a constant magnetic field of 10 mT either in the substrate plane or perpendicular to it. The spectra were normalized to the incoming photon flux using the drain current from the last refocusing mirror upstream from the measuring chamber and the corresponding spectra measured at the clean substrate. Unless indicated in the text, the spectra were then scaled to zero in the pre-edge energy region.

In order to study separately the magnetization of both layers, grazing and normal incidence geometries were used for in-plane and out-of-plane magnetized substrates using left- and right-circularly polarized light with angles of θ = 70° and 0° between the wave vector **k** and the surface normal, respectively.

The orientation of the deposited molecules was determined by angular-dependent near-edge x-ray-absorption fine structure (NEXAFS) spectra at the N- and C-K edges for molecules on both ferromagnetic film substrates (Co, Ni). The NEXAFS spectra indicate that the deposited molecules are lying almost flat on the surface with the plane of the four N atoms aligned parallel to the substrates.[18] Apart from determining the orientation of the deposited molecules, the N-K edge is a sensitive indicator for perturbations of the molecule that might occur during the adsorption process or due to radiation damage. Our N-K edge spectra exhibit all fine structures that were observed and discussed for a similar molecule Zn-tetraphenylporphyrin,[5] implying that the coordination plane around the Fe atom stays intact during measurements. Similar spectra collected with ten times lower photon flux density exhibited the same features for all the absorption edges. From this, we conclude that radiation-damage effects are not important for the spectra shown here. An explanation could be that the π ring of the porphyrin molecule, in proximity to the metallic substrate, strongly stabilizes the entire molecule, making it less sensitive to radiation damage.[19] However, we could not detect any edge jump in the energy range of the Cl-$L_{2,3}$ edges. Density functional theory (DFT) calculations[18] showed that the ferromagnetic coupling for the molecules to the substrate occurs only when the Cl atom is detached. This would imply a reduction of the Fe valence state. In order to clarify this, we carried out measurements on a bulk sample, prepared by stamping Fe(III)-OEP-Cl powder onto an indium foil. When comparing the Fe-$L_{2,3}$ x-ray-absorption (XA) spectra for a Fe-porphyrin submonolayer on Co/Cu(100) to the one of the bulk sample, shown in Fig. 1(a), an ~1.3 eV shift to lower energies is observed. This shift indicates a stronger screening of the initial and final states, concomitant with an increase of charge at the Fe atom,[20–22] leaving the Fe atoms in a predominantly divalent state. On the other hand, such a valence state can also be originated by Fe-ligand charge transfer back-bonding and back donation mechanisms,[9] possibly triggered by the underlying metallic surface.
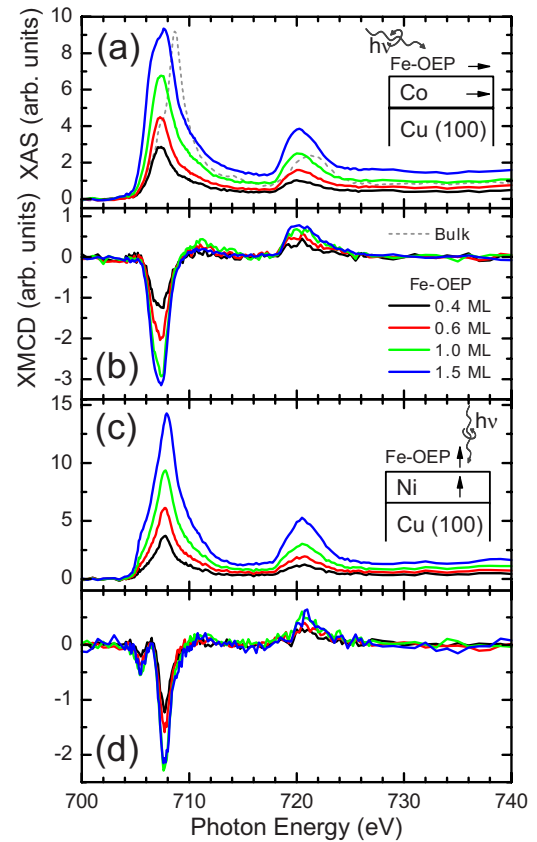

FIG. 1. (Color online) Fe-$L_{2,3}$ XAS and XMCD spectra recorded at room temperature for different coverages of Fe-porphyrin molecules [(a) and (b)] on 5 ML Co/Cu(100) and [(c) and (d)] on 15 ML Ni/Cu(100). Panel (a) includes the XAS data of Fe-OEP-Cl bulk.

III. RESULTS AND DISCUSSION

We have studied the differences in molecule-substrate interactions for different Fe-porphyrin coverages and substrates by means of XAS and XMCD. Figure 1 shows, from top to bottom, the Fe-$L_{2,3}$ helicity-averaged XAS and XMCD spectra taken for thicknesses t = 0.4, 0.6, 1.0, and 1.5 ML on Co [panels (a) and (b)] and Ni [panels (c) and (d)] magnetically saturated substrates, measured at room temperature from a series of consecutive deposition. In order to stress the thickness dependence of the white lines and the edge jumps, the shown XA spectra were only normalized to the pre-edge region. It should be noted that the same angular dependence of the N-K XAS signals was found for the four thicknesses, proving that the molecules are always lying flat on the substrate. In the case of the XMCD, the spectra were obtained as the difference of either the corresponding XAS signals for left- and right-circularly polarized light or the spectra obtained by inverting the direction of the external magnetic field. Due to the in-plane and out-of-plane magnetic easy axes for Co and Ni, the respective spectra were measured at grazing and normal incidences, respectively, as indicated by the insets in panels (a) and (c).

In the case of the Co substrate, the two Fe-$L_{2,3}$ white lines are relatively broad, resembling the analogous spectra for
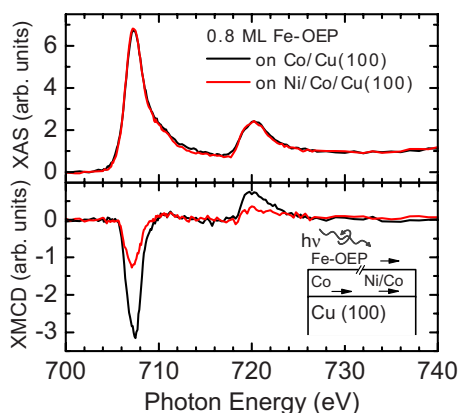
FIG. 2. (Color online) Fe-$L_{2,3}$ XAS and XMCD spectra of 0.8 ML Fe-OEP molecules deposited on 5 ML Co/Cu(100) (black) and on 5 ML Ni/5 ML Co/Cu(100) (red) substrates. All spectra were recorded at room temperature.

bulk metallic materials. For thicknesses t smaller or of the order of 1 ML, the intensity increases with t and no different line shapes are observed. On the contrary, the L_3 signal for $t=1.5$ ML displays a broader feature where two peaks can be guessed. This can be explained by the different ligand fields around the Fe atom present in the first molecular layer, in direct contact to the substrate, and the second layer. In the latter, only weaker intermolecular interactions can be envisaged on the bottom side of the molecule, while the top side faces the vacuum. Furthermore, the corresponding XMCD signals again show a quasimetallic shape and decrease in relative intensity for increasing thicknesses.

The Fe-$L_{2,3}$ XA spectra for the Ni substrate case [Fig. 1(c)] show a very different line shape. Both edges display narrow peaks at $E=708$ and 720.5 eV, each with two shoulders at lower and higher photon energies. No clear thickness dependence is observed in the line shapes. The XMCD signal is characterized by a narrow peak at $E=707.6$ eV preceded by a small feature at $E=705.5$ eV; these features are reproduced in the L_2 edge.

The explanation of the different line shapes for the Co and Ni substrates does not lie on a substrate-dependent hybridization mechanism but on purely geometrical reasons: The different experimental geometries (grazing and normal incidences for Co and Ni, respectively) probe different unoccupied Fe 3d orbitals. This is readily proven by comparing the spectra taken on Co and Ni for the same geometry. By preparing a 5 ML Ni film on a 5 ML Co film, the Ni magnetization is forced to the in-plane direction by the Co film. As can be seen in Fig. 2, the Fe-$L_{2,3}$ XAS and XMCD spectra of 0.8 ML Fe-OEP on Co and Ni measured at grazing incidence show exactly the same line shape.

In order to understand these differences in spectral shape, we need to consider the electronic transition process in transition metals. In contrast to the higher energy K edges, the soft x-ray $L_{2,3}$ absorption spectrum cannot be described by the simpler one-electron model. Instead, all the partially empty levels of the atom contribute in the calculation of the quantum numbers of the initial $3d^N$ and final $2p^5 3d^{N+1}$ states. These states are subject of the various interactions such as

Coulomb repulsion, spin orbit, and the ligand field created by the neighboring atoms. All these terms provoke successive changes in the energy diagrams of the electronic states, resulting in a plethora of possible transitions from the initial to the final states, the so-called atomic multiplets. Although computer-assisted calculation methods[23,24] are available to produce theoretical spectra of metallorganic complexes,[25] these methods have been proven insufficient for the case of more complex metallorganic molecules, where orbital hybridization and σ and π bonding and back-bonding effects play an important role, requiring the addition of DFT methods to fit the experimental results.[8,9]

Despite these difficulties, we will try to find out which 3d orbitals are probed in the two geometries. Taking into consideration the four coplanar N atoms around the Fe, the ligand field presents a D_{4h} symmetry. This lifts the degeneracy of the e_g and t_{2g} orbitals, proper under a cubic symmetric field, resulting in different energies for the d_{z^2}, $d_{x^2-y^2}$, d_{xy}, and d_π orbitals (d_π is the result of hybridizing d_{xz} and d_{yz}). Based on DFT calculations,[10] we will assume that the ground state configuration of the Fe-OEP molecule is $(d_{xy})^2(d_{z^2})^2(d_\pi)^2$, corresponding to the $^3A_{2g}$ state and displaying an intermediate spin $S=1$. This leaves two empty states in the $d_{x^2-y^2}$ orbital and another two in the d_π orbital, i.e., the latter is half filled. By considering the projection of the different orbitals with respect to the polarization of the incoming light in the grazing and normal geometries, we obtained that, for normal incidence, the $d_{x^2-y^2}$ orbital is weighted twice as strong as d_π, whereas for grazing incidence, the weighting factor becomes 0.8. We can thus conclude that the missing spectral features for normal geometry are mostly related to the d_π orbital.

We turn now our attention to the element-specific magnetic properties by investigating the XMCD spectra shown in Fig. 1. A clear XMCD signal for all coverages shows that the paramagnetic porphyrin molecules deposited on both ferromagnetic films are magnetically ordered. Furthermore, the XMCD signals for all coverages and both substrates are negative at the L_3 edge, as the Co and Ni XMCD signals (not shown), demonstrating that the molecule-substrate coupling is ferromagnetic. From element-specific hysteresis loops of the Fe-, Co-, and Ni-L_3 XMCD intensities (not shown here), it is evident that the orientation of the Fe spin switches along with the spins of the ferromagnetic films and that there exists a ferromagnetic exchange coupling of the Fe moments of the porphyrin molecules to the magnetic substrate.

The magnetic properties of Fe-porphyrin molecules can be understood more clearly from Fig. 3, where the integrated intensities of the Fe-L_3 XMCD signal normalized to the white line, shown in Fig. 1, are plotted as a function of coverage for Co and Ni. The values obtained at the lowest coverage are normalized to unity in both cases. It can be seen that the magnetic signal of the deposited Fe-porphyrin molecules originates mostly from the first molecular layer only: on Co, the ratio remains constant (within the error bars) for 0.4 and 0.6 ML and only decreases for films thicker than ∼1 ML. In the case of Ni, the XMCD/XAS ratio decreases monotonically with thickness, suggesting a weaker substrate-molecule coupling as compared to the Co case. The origin of the magnetic ordering is discussed in detail in our recent
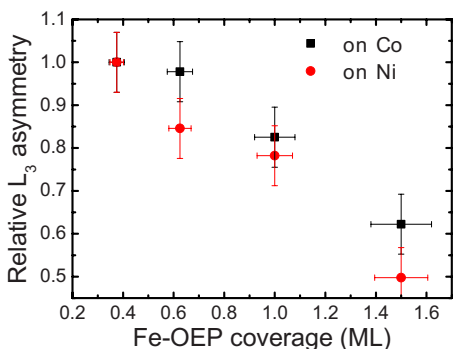
FIG. 3. (Color online) Fe-OEP coverage dependence of the integrated intensities of Fe-L_3 XMCD normalized to the white line on 5 ML Co/Cu(100) (black) and 15 ML Ni/Cu(100) (red) substrates. The values obtained at the lowest coverage are normalized to unity in both cases.

work.[18] By using the *ab initio* electronic structure calculations, it has been shown that the ordering is not due to a direct exchange interaction between Fe and Co. Instead, a 90° ferromagnetic exchange mechanism through the N ligands is found to be responsible for the coupling. In order to compare with theoretical coupling energies, we also measured the temperature dependence of the XAS and XMCD signals.

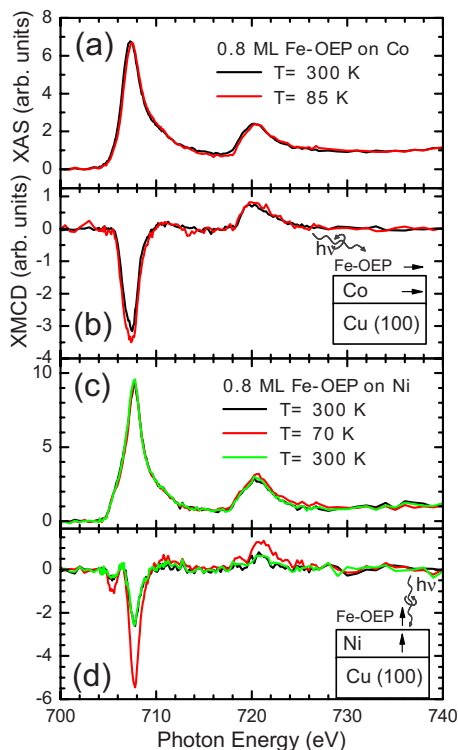Figure 4 shows the XAS and XMCD Fe-$L_{2,3}$ spectra recorded at 300 and ∼80 K for 0.8 ML coverage of Fe-

FIG. 4. (Color online) Fe-$L_{2,3}$ XAS and XMCD spectra for 0.8 ML Fe-OEP molecules [(a) and (b)] on 5 ML Co substrate recorded at 300 and 85 K and [(c) and (d)] on 15 ML Ni at 300, 70, and 300 K.
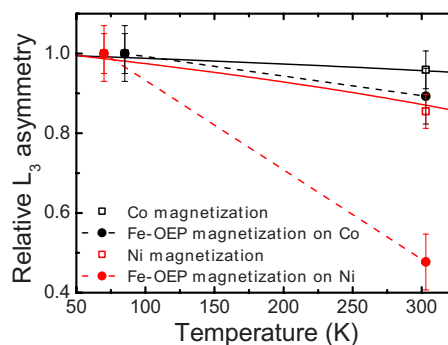

FIG. 5. (Color online) Temperature dependence of the Fe, Co, and Ni magnetizations obtained from integrated XMCD signals normalized to the corresponding white lines. The signals obtained at low temperatures have been normalized to unity. Full lines represent $M(T)$ for Co and Ni as obtained from mean field approximation. The dashed lines serve as guides to the eye.

porphyrin molecules on Co and Ni substrates. Whereas the integrated XAS intensity does not show any noticeable change in the two cases for the two temperatures, the XMCD amplitude does vary with T. Furthermore, any temperature-dependent change is fully reversible, as can be seen in Fig. 4(d) for both the XAS and the XMCD spectra when they were successively recorded at 300, 70, and then again at 300 K. Other than scaled by a common factor, all the spectral features found at 300 K, explained above in detail, remain at low temperatures.

In order to discern the temperature-dependent magnetic properties of the molecules from the temperature-dependent magnetization of the substrates, we have plotted in Fig. 5 the integrated Fe-, Co-, and Ni-L_3 XMCD signals, shown in Fig. 4, normalized to the white lines as a function of temperature, scaled to the signals at low temperatures. These signals are basically proportional to the magnetization of each element. The Curie temperatures of 5 ML Co and 15 ML Ni films are reported to be around 850 K (Ref. 26) and 550 K,[27] respectively. This explains the slightly larger reduction in Ni XMCD signal as compared to that of Co. This can also be seen by the two solid curves, which are drawn using the mean field approximation and serve as guides to the eye.

Regarding the Fe magnetization on Co, it follows that of the substrate by decreasing ∼10% at 300 K. In contrast, the Fe XMCD on Ni shows a much larger reduction of ∼50% than the one of the Ni magnetization. This difference of the Fe XMCD signal of molecules deposited on Ni as compared to Co indicates the presence of different coupling strengths in the two cases. The weaker coupling strength in the case of Fe-OEP on Ni also supports the indirect coupling mechanism found by theory.[18] However, it should be noted that, on the basis of our experimental techniques, we cannot distinguish between a direct or indirect coupling mechanisms. On the other hand, if the Fe ion detached from the molecule and adsorbed directly on the underlying film, it would be expected that the Fe magnetization should follow the $M(T)$ curve of the film. This is not the case, indicating that the Fe ion remains at the center of the porphyrin ring.

In order to get a first-approximation value of the exchange coupling energy E_c between the substrate magnetization and

the Fe spin, we assume a Brillouin function with a total angular momentum quantum number $J=1$ to model the temperature dependence of the Fe magnetization. We determine that $E_c = 0.07$ and 0.02 eV for the Co and Ni cases, respectively. The value for Co is of the same order of magnitude as the one calculated by DFT-GGA+U [$E_c = 0.05$ eV (Ref. 18)]. Within the limitations of this approach, we conclude that a much larger coupling appears between the Fe spin when the molecule is on Co as compared to the Ni substrate. The larger coupling for Co can be addressed either to an intrinsic effect of the substrate or to its magnetization direction. In view of the Fe-$L_{2,3}$ spectra shown in Fig. 2 for Co and Ni/Co substrates, both with in-plane magnetization, we observe that the Fe-XMCD signal on the Ni/Co is approximately half of that on Co, with almost the same XAS intensity. Thus, the weaker coupling of Fe-porphyrin molecules to the Ni substrate is not related to the different magnetization directions but to the electronically different surfaces. As a possible explanation for the reduced coupling energy in the Ni case, we can consider the 60% smaller magnetic moment of Ni surfaces as compared to the Co ones.[28,29] However, the extent of this effect can be modified by the presence of the molecules adsorbed on the surfaces.[30]

Furthermore, we make use of the XMCD sum rules to calculate the effective Fe spin moment at 70 K (including the magnetic dipole term $\langle T_z \rangle$). We obtain that μ_S^{eff}(Fe) $= 0.65 \pm 0.1$ and $0.45 \pm 0.1 \mu_B$/hole for molecules deposited on Co and Ni films, respectively. The relatively large error bar is due to the fact that the molecular coverage of ~ 1 ML corresponds to an effective Fe coverage in the $1/100$ ML range. Despite this, if we assume four holes in the Fe $3d$ orbitals, these values agree with the $S=1$ of the calculated $^3A_{2g}$ initial state. The ratio of orbital to effective spin moment is found to be $\mu_L / \mu_S^{eff} \sim 5-10$ %, indicating that the orbital moment is nearly quenched. The exchange coupling between porphyrin molecules and Co is much stronger, and therefore, in this case, the exchange coupling energy is greater than the thermal energy. On the other hand, a comparatively weak coupling of porphyrin molecules to the Ni substrate may account

for more prominent temperature-dependent effects. A detailed theoretical study of the electronic structure of these molecules on two different ferromagnetic substrates would help put forward more quantitative arguments to explain the experimental observations.

IV. CONCLUSIONS

The present study describes systematic XAS and XMCD measurements on ultrathin Fe-porphyrin molecular layers deposited on epitaxially grown ferromagnetic films on Cu(100). After evaporation, the molecular plane remains intact and lies flat on the substrates. Strong spectral differences that appear in the XAS and XMCD signals are not substrate dependent but arise purely from geometrical considerations, since the incoming x-ray beam at grazing and normal incidences probes different Fe $3d$ orbitals.

It is shown that only the molecules that are in close vicinity to the ferromagnetic substrate are magnetically ordered. From the temperature dependence of the Fe and substrate magnetizations, the coupling strengths for both substrates are calculated, yielding a much stronger coupling to the Co substrate than to Ni. The experimental value for the coupling with Co agrees well with results from DFT calculations on the same system. The XMCD sum rule analysis yields an Fe spin moment that also depends on the subjacent substrate. Being somewhat higher for Co, it agrees with the intermediate-spin state calculated for these molecules.

*Permanent address: Surface Physics Laboratory, Fudan University, Shanghai 200433, People's Republic of China.

†Corresponding author; FAX: +49 203 3793601; heiko.wende@uni-due.de

‡Permanent address: Department of Physics, IIT Delhi, Hauz Khas, New Delhi 110016, India.

[1] H. Kalish, J. E. Camp, M. Stępień, L. Latos-Grażyński, M. M. Olmstead, and A. L. Balch, Inorg. Chem. **41**, 989 (2002).

[2] T. Lukasczyk, K. Flechtner, L. R. Merte, N. Jux, F. Maier, J. M. Gottfried, and H.-P. Steinrück, J. Phys. Chem. C **111**, 3090 (2007).

[3] T. Okajima, Y. Yamamoto, Y. Ouchi, and K. Seki, J. Electron Spectrosc. Relat. Phenom. **114-116**, 849 (2001).

[4] G. Polzonetti, V. Carravetta, G. Iucci, A. Ferri, G. Paolucci, A. Goldoni, P. Parent, C. Laffon, and M. V. Russo, Chem. Phys. **296**, 87 (2004).

[5] S. Narioka, H. Ishii, Y. Ouchi, T. Yokoyama, T. Ohta, and K. Seki, J. Phys. Chem. **99**, 1332 (1995).

[6] A. Scheybal, T. Ramsvik, R. Bertschinger, M. Putero, F. Nolting, and T. A. Jung, Chem. Phys. Lett. **411**, 214 (2005).

[7] A. Ghosh, E. Gonzalez, T. Vangberg, and P. Taylor, J. Porphyr. Phthalocyanines **5**, 345 (2001).

[8] R. K. Hocking, E. C. Wasinger, F. M. F. de Groot, K. O. Hodgson, B. Hedman, and E. I. Solomon, J. Am. Chem. Soc. **128**, 10442 (2006).

[9] R. K. Hocking, E. C. Wasinger, Y.-L. Yan, F. M. F. de Groot, F. A. Walker, K. O. Hodgson, B. Hedman, and E. I. Solomon, J. Am. Chem. Soc. **129**, 113 (2007).

[10] M.-S. Liao and S. Scheiner, J. Chem. Phys. **116**, 3635 (2002).

[11] M.-S. Liao and S. Scheiner, J. Chem. Phys. **117**, 205 (2002).

[12] H. Wende, Rep. Prog. Phys. **67**, 2105 (2004).

[13] J. V. Barth, G. Costantini, and K. Kern, Nature (London) **437**,

671 (2005).

[14] P. M. Panchmatia, B. Sanyal, and P. M. Oppeneer, in *Applied Parallel Computing. State of the Art in Scientific Computing*, edited by B. Kågström *et al.*, Lecture Notes in Computer Science Vol. 4699 (Springer-Verlag, Berlin, Heidelberg, 2007), pp. 502–509.

[15] B. T. Thole, P. Carra, F. Sette, and G. van der Laan, Phys. Rev. Lett. **68**, 1943 (1992).

[16] P. Carra, B. T. Thole, M. Altarelli, and X. Wang, Phys. Rev. Lett. **70**, 694 (1993).

[17] A. Scherz, H. Wende, C. Sorg, K. Baberschke, J. Minár, D. Benea, and H. Ebert, Phys. Scr., T **T115**, 586 (2005).

[18] H. Wende, M. Bernien, J. Luo, C. Sorg, N. Ponpandian, J. Kurde, J. Miguel, M. Piantek, X. Xu, P. Eckhold, *et al.*, Nat. Mater. **6**, 516 (2007).

[19] B. Barbiellini and P. M. Platzman, New J. Phys. **8**, 20 (2006).

[20] F. M. F. de Groot, J. C. Fuggle, B. T. Thole, and G. A. Sawatzky, Phys. Rev. B **42**, 5459 (1990).

[21] A. S. Vinogradov, A. B. Preobrajenski, S. A. Krasnikov, T. Chassé, R. Szargan, A. Knop-Gericke, R. Schlögl, and P. Bressler, Surf. Rev. Lett. **9**, 359 (2002).

[22] W. M. Heijboer, A. A. Battiston, A. Knop-Gericke, M. Hävecker, R. Mayer, H. Bluhm, R. Schlögl, B. M. Weckhuysen, D. C. Koningsberger, and F. M. F. de Groot, J. Phys. Chem. B **107**, 13069 (2003).

[23] R. D. Cowan, *The Theory of Atomic Structure and Spectra* (University of California Press, Berkeley, 1981).

[24] B. T. Thole, G. van der Laan, J. C. Fuggle, G. A. Sawatzky, R. C. Karnatak, and J.-M. Esteva, Phys. Rev. B **32**, 5107 (1985).

[25] C. Cartier dit Moulin, P. Rudolf, A. M. Flank, and C. T. Chen, J. Phys. Chem. **96**, 6196 (1992).

[26] P. Bruno, in *Magnetic Thin Films, Multilayers and Surfaces*, MRS Symposia Proceedings No. 231 (Materials Research Society, Pittsburgh, 1992), p. 299.

[27] K. Baberschke, Appl. Phys. A: Mater. Sci. Process. **62**, 417 (1996).

[28] A. Ney, A. Scherz, P. Poulopoulos, K. Lenz, H. Wende, K. Baberschke, F. Wilhelm, and N. B. Brookes, Phys. Rev. B **65**, 024411 (2001).

[29] A. Ney, K. Lenz, P. Poulopoulos, and K. Baberschke, J. Magn. Magn. Mater. **240**, 343 (2002).

[30] T. Yokoyama, K. Amemiya, M. Miyachi, Y. Yonamoto, D. Matsumura, and T. Ohta, Phys. Rev. B **62**, 14191 (2000).